Materials Physics and Mechanics 11 (2011) 157-182 Received: April 25, 2011

CREEP LIFE DESIGN CRITERION AND ITS APPLICATIONS TO PRESSURE VESSEL CODES

Jad Jelwan[1*], Mahiuddin Chowdhury[2], Garth Pearce[1]

[1]Department of Mechanical and Manufacturing Engineering,

University of New South Wales, Sydney, NSW 2052, Australia

[2] Department of Naval Architecture, School of Mechanical and Manufacturing Engineering,

University of New South Wales, Sydney, NSW 2052, Australia

*e-mail: jad.jelwan@unsw.edu.au

Abstract. Pressure vessels equipment is used in the oil, chemical, nuclear power plant and many other industries. Life prediction of such components subjected to high temperature is very important to avoid the catastrophic consequences of failure. The designer often works to the requirements of a standard or code of practice. In mentioning codes and standards, one should also mention that in many nations there is a national organization which develops such standards. In France, there is the RCC-MR practice code for creep design; the R5 from the British Energy, and many other methods proposed by the European Creep collaborative Committee (ECCC) and the National Institute of Material Science (NIMS) in Japan. However, the major shortcomings of the abovementioned standards, they are not practical to use or/and too conservative which involves many other considerations such as economics, safety and manufacturing problems. This paper describes a relatively pragmatic and accurate paradigm for predicting the lives of such components. The application of the proposed paradigm to an internally pressurized vessel shows that the elastic-plastic-creep life of the component can be predicted with an error of less than 10 %.

1. Introduction

Creep problems are not new. It appeared in the last century and many applications and phenomenon-logical proposals have been developed at the end of the 19th century. For Instance, Schweiker [1] dealt with pressurized thick-walled tubes; a problem which will seems to provoke interest and becomes important to meet strict requirements for safe operation with a primary attention for creep deformation. In the beginning of the 20th century real practical problems were required to investigate the behavior of the material subjected to high temperature and constant load where creep analysis appeared to be an important and independent division beyond the engineering mechanics and stress/strain analysis in generalizing information from experimental observations and numerical investigations as structures and machines have been expected to operate at higher temperatures in order to achieve greater efficiencies. An enormous effort has been put into phenomenon-logical studies of the uniaxial creep test and a number of misunderstandings have been produced since those methods are based on assumptions considering that the deformation to be as a function of stress only, which leads to an inadequacy for the description of creep behavior. Also, as Wilshire and Scharning [2] pointed out, creep lives are governed by the accumulations of strains and therefore the methods that take into account stress values only may not result in valid predictions. Although many theories have been proposed in an attempt

to account for the plastic flow of the metals under stress at elevated temperatures, all extant theories appear to deviate from the experimental facts. In principle it is possible to determine the distributions of stress and strain throughout a structure provided the constitutive laws for the material from which the structure is made are known. However, the physical examination of plasticity with the interaction of creep is not well developed. It might be an exaggeration to call it "not well developed", but it is common practice today to base an engineering design on laboratory tests conducted under conditions remote from the operating conditions, using complicated design calculations that are predicated on naive and often erroneous assumptions. Therefore, it is difficult to envisage how simple yet all embracing constitutive laws which could be used in any design procedure could ever be formed. While a considerable amount of attention has been given to the general subject of creep of metals, most of the effort has been devoted to the case of uniaxial load and uniaxial stress of a tensile specimen at a constant temperature a confusing number of creep laws have been basis, which creates a little comfort to the designer working with materials at high temperature, since he would like to predict, with some degree of reliability, the creep behavior of complex and expensive machine parts. None seems to be entirely satisfactory and few have any physical basis. In view of the difficulties in performing even the uniaxial creep test, and the hopeless of trying to amass sufficient data to cover all design eventualities, this paper aims to examine which method can yield the information of greatest significance. Also, one of the as yet unresolved engineering problems is forecasting the creep lives of weldement in a pragmatic way with sufficient accuracy. There are number of obstacles to circumvent including: complex material behavior, lack of accurate knowledge about the creep material behavior especially about the heat affected zone (HAZ), accurate and multi-axial creep damage models, etc. Furthermore, weld joints represent particularly features for steel structural components operating at relatively high temperatures, even in the absence of typical welding defects. As a matter of fact, these regions are characterized by the presence of a wide range of microstructures that can be summarized in a base metal structure, a weld metal and a set of graded microstructures within the heat affected zone. Each microstructural region is characterized by its proper short and long term high temperature mechanical behavior, this latter being related to both the initial 'local' microstructure and to its high temperature microstructural evolution. In addition, the combination of material, loading conditions and geometry in weld joint can lead to the presence of complex stress states and to local constraint that were found to be of great importance in causing the reduction of creep life of weld joints [3, 4]. There are several macroscopic models for creep life forecasting, including time-fraction rule, strain fraction rule, the reference stress, skeletal stress method, continuum damage model, etc. Each of which has their own limitations. This paper gauges to a multi-axial yet pragmatic and simple model for creep life prediction operating at high temperature and subjected to an elastic-plastic-creep deformation.

2. Creep Life Assessment Methods

2.1. Reference Stress Method. The reference stress method describes the inelastic response of structures. The method has been developed to enable simplified assessment procedures to be produced for both defect-free and defective components [5, 6]. When the reference stress is used in conjunction with uniaxial creep rupture data of the material of the component, the creep life of the component can be determined. It is usually computed, using the limit load (P_L) of the component where:

$$\sigma_{ref} = \frac{P\sigma_y}{P_L}. \tag{1}$$

However, equation (1) is derived based on the lower bound theorem and underestimates the true σ_{ref} and therefore it could result in non-conservative life predictions. To alleviate this shortcoming problems, Sim [7] derived a simple equation by assuming that the reference stress is responsible for creep rupture, which is a function of the principal stress and the equivalent stress using the skeletal stress concept.

$$(\sigma_r)_{ref} = \alpha(\sigma_1)_{ref} + (1-\alpha)(\sigma_e)_{ref}. \tag{2}$$

The major shortcoming of Eq. (2) is that the determination of the reference stress is thought to be somewhat approximated. For instance, α is not known and its evaluation requires expensive creep testing of the component and it is time consuming and usually impractical. In practice, the analyst either assumes $\alpha = 1$ resulting in $\sigma_r = \sigma_e$ or $\alpha = 0$ resulting $\sigma_r = \sigma_1$ which adds to the analysis an inaccuracy of the predicted creep life. In addition, Marriot and Leckie [8] showed that the skeletal point method is applicable for a limited number of engineering structures. A potential function of the form defined by von Mises is used to obtain a reference stress (S) for the tube and which is given as [9]:

$$S = \frac{\sqrt{3}}{2} \times K \times \frac{P_e}{\ln\left(\frac{d+H}{d-H}\right)}. \tag{3}$$

Here d and H are the tube mean diameter and thickness at any time t and K is a constant that depends on the geometry of the tube area which is being thinned and it is usually assumed to be equal to 1. However, this conservative assumption is thought to have some practical aspects embedded in it because, in practice, it is usually difficult to determine the geometry of the pits precisely [9].

2.2. R5 Life Assessment Method. The R5 is the procedure for the assessment of high temperature components where creep becomes significant [10]. The calculations in R5 are based largely on simplified methods of stress analysis. This is a compromise between the pessimism of using elastic analysis and the cost and complexity of inelastic computation [10]. The simplified method is the so-called reference stress technique. Issue 2 of R5 contains seven Volumes [11].

Volume 1 presents an overview of the code;

Volume 2 analyses and assesses the methods for defect free structures;

Volume 3 evaluates the creep-fatigue crack initiation;

Volume 4 appraises the assessment procedure for dissimilar metal welds;

Volume 5 reviews the creep-fatigue crack growth;

Volume 6 reassesses the procedure for dissimilar metal welds;

Volume 7 provides guidance for the behaviour of similar welds subjected for steady creep loading of CrMoV pipe work components.

In this paper, Volume 2 and Volume 7 have been explored for creep assessment; reference stress is used to calculate the creep strain (creep damage). The reference stress for defect free cylinder is based on the maximum difference between principal stresses where the hoop stress is dominant and it is given as [11, 12]:

$$\sigma_{ref,uh} = \frac{P}{P_L}\sigma_y, \tag{4}$$

where $P_L = \ln(r_0 / r_i)\sigma_y$.

For a welded pressurized vessel, a weld stress redistribution factor denoted as k is introduced taking into account the variation of the creep strain rates between the PM, HAZ and which could be present in WM too. The accumulation of strain within the PM takes control of the vessel behavior when it is loaded by internal pressure causing a hoop stress state domination. Hence the creep rupture reference stress is given as:

$$\sigma_{ref,h}^{rup} = k\sigma_{ref,uh}, \tag{5}$$

where k is the stress redistribution factor of 1.235 in a mixed HAZ [12].

2.3. RCC-MR Creep Life Assessment (French Code). According to the general design rules of RCC-MR class 2 piping rules has implemented the ASME section III and extended to the creep regime [13]. This code is applicable to the components subjected at high temperature. The RCC-MR is divided into five sections defined as follows [13]:

-Section I provides sets of design rules for various types of components;

-Section II contains procurement specifications for parts and products which can be used for components design;

-Section III is devoted to rules for applying the various destructive and non destructive examination methods;

-Section IV gives the rules relating to the various qualifications for welding operations and welding procedures;

-Section V provides rules relating to manufacturing operations other than welding.

For life prediction of components subjected to high temperature, RCC-MR recommend to apply the multiaxial creep damage assessment criteria using the equivalent stress (σ_{eq}) as a function of the von Mises stress (σ_{vM}) and the hydrostatic stress (σ_H) and it is given as [14]:

$$\sigma_{eq} = 0.867\sigma_{vM} + 0.4\sigma_H, \tag{6}$$

where

$$\sigma_{vM} = \frac{1}{\sqrt{2}}[(\sigma_\theta - \sigma_1)^2 + (\sigma_1 - \sigma_R)^2 + (\sigma_R - \sigma_\theta)^2]^{\frac{1}{2}}. \tag{7}$$

Here σ_θ, σ_1, and σ_R are the computed hoops, longitudinal and radial stress respectively:

$$\sigma_\theta = \frac{PD_m}{2h}, \tag{8}$$

$$\sigma_1 = \frac{PD_m}{4h}, \tag{9}$$

$$\sigma_R = \frac{-P}{2}. \tag{10}$$

In order to establish the rupture time the ECCC (see Section 4.1) and NIMS (see Section 4.2) are used to compute the life of each component based on the rupture stress calculated above. It should be noted, RCC-MR recommend the use of a weld strength factor of 0.9 [14] when dealing with weld.

2.4. European Creep Collaborative Committee (ECCC) Life Assessment. The creep rupture strength of 0.5Cr-0.5Mo-0.25V steel is shown in Fig. 1. The analysis from which the data in Fig. 1 was carried out as part of the activities of the European Creep Collaborative Committee and additional details can be found from their published data sheets [15]. The distribution of test durations is shown in Table 1.

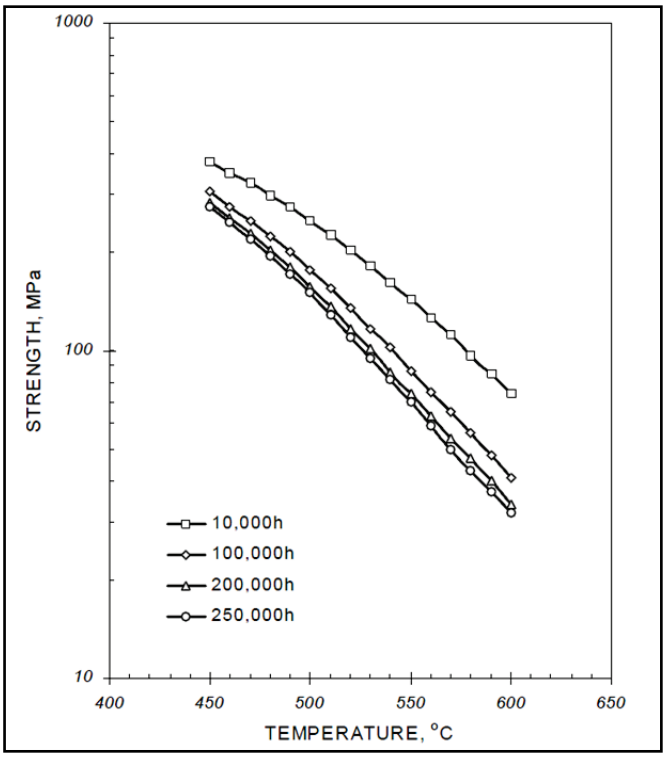

Fig. 1. Creep ruptures strength data of 0.5Cr-0.5Mo-0.25V [15].

The data were assessed using the BS PD6605 procedure and the following master equation was derived as:

$$\ln\ln\left(t_u^*\right) = \beta_0 + \beta_1 \log\log\left(\sigma\right) + \beta_2\sigma^2 + \beta_3\sigma^2 + \beta_4 T + \beta_5 / T\,, \tag{11}$$

where t_u^* the predicted rupture time in hours, T is the absolute temperature, and σ is the stress in N mm^{-2}.

Table 1. The constants β_i for equation (11) [15].

β_0	-39.765870
β_1	-843513298
β_2	-0.00186616660
β_3	$-2.91037377 \cdot 10^{-0.5}$
β_4	0.00935613085
β_5	49662.4102

As for the 2.25Cr-1Mo steel is widely used as tubes for boilers and heat exchangers and as components for pressure vessels. Creep rupture data of 2.25Cr-1Mo steel tubes was

analyzed using the Manson-Haferd parameter method [15]. The master rupture curve obtained is shown in Fig. 2.

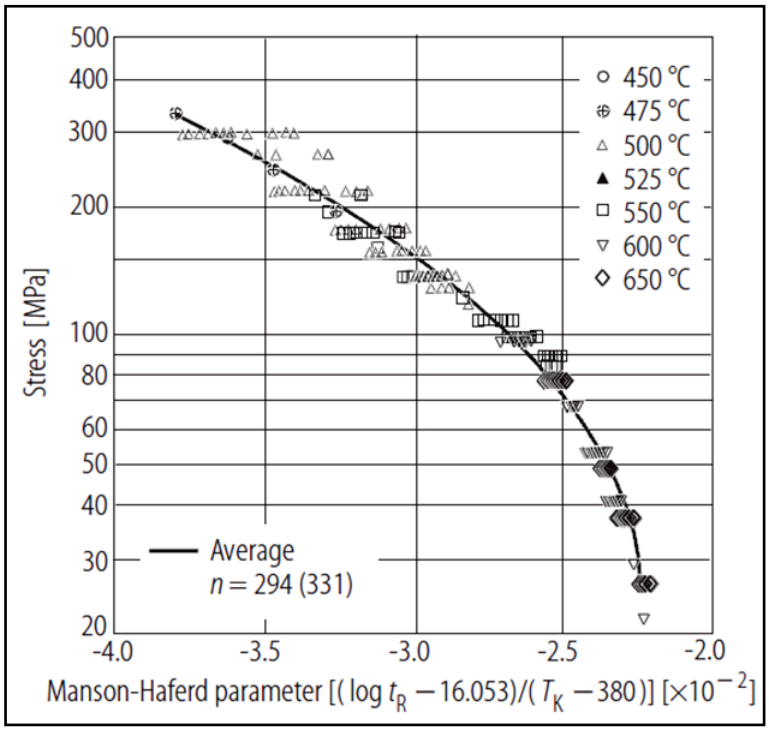

Fig. 2. Creep ruptures strength data of 0.5Cr-0.5Mo-0.25V [15].

2.5. National Institute for Materials Science, Materials Database Station (NIMS). Using the NIMS creep data sheet number 20B and 3B one can find the material properties of 0.5Cr-0.5Mo-0.25V steel tubes for boilers and heat exchangers. From Table 2 the regression equation for isothermal creep-rupture data is given, where the constants c_0, c_1, and c_2 at 565 °C. For 0.5Cr-0.5Mo-0.25V and 2.25Cr-1Mo steels the regression equation is given as [16]:

$$\log t_r = c_0 + c_1\left(\log \sigma_r\right) + c_2(\log \sigma_r)^2 . \tag{12}$$

Table 2. Creep Rupture Data Summary for the regression form equation extrapolated at 565°C [16].

Material Type	c_o	c_1	c_2
2.25Cr-1Mo steel	2.177314	8.9897337	-3.1204188
0.5Cr-0.5Mo-0.25V steel	-3.728122	11.63370	-3.837675

3. Proposed Method based on The Exhaustion of Strain Energy Density

Recently Zarrabi and Jelwan [17, 18] proposed a new paradigm which allows the material to undergo elastic-plastic-creep deformation but it postulates that the dominant damage mechanism is creep and at the point of failure the component fails by excessive creep deformation and/or creep rupture. This allows limited plastic deformation at the stress-concentration regions, which as mentioned above has practical significance, as the plastic deformation in the properly designed components is normally limited to the stress-concentration regions. Consider a component that is subjected to several loads. These loads

are increased in their respective magnitudes from zero to their operational levels over relatively short period of time so that it can be assumed that at time $t = 0$ they instantly cause elastic deformation only in the regions where the corresponding equivalent stresses are below the yield strength and plastic deformation in the regions where the equivalent stresses are above the yield strength. Having reached their respective operational levels, the loads are taken to be constant causing creep damage/deformation until the point of failure. It is also assumed that the material temperature (T) is uniform and constant so that there is basically no fatigue damage. In the following, the superscript e refers to elastic, p refers to plastic and c refers to creep. At the time t the rate of the total internal energy density (i.e., the rate of the total internal energy per unit of the volume), dW may be expressed in terms of stress (σ_{ij}) and strain rate ($\dot{\varepsilon}_{ij}^{k}$) components as:

$$d\dot{W} = \sigma_{ij}\left(\dot{\varepsilon}_{ij}^{e} + \dot{\varepsilon}_{ij}^{p} + \dot{\varepsilon}_{ij}^{c}\right) + \dot{W}_{t}, \tag{13}$$

where $\dot{W}_t$ is the rate of the internal (thermal) energy in the absence of stress at a point in the material. The total internal energy density at any point can be calculated by integrating Eq. (13) with respect to time:

$$W = \left\{\iint\left[\sigma_{ij}(\dot{\varepsilon}_{ij}^{e} + \dot{\varepsilon}_{ij}^{p} + \dot{\varepsilon}_{ij}^{c})\right]dt + \iint \dot{W}_{t}\, dt\right\}. \tag{14}$$

Note that the second term in Eq. (13), i.e., $W_t = \iint \dot{W}_t\, dt$ is the input thermal energy density and it accounts for microstructural damages in the absence of stress. It may be calculated analytically for simple cases or numerically using the finite element method (FEM) for more complex cases. Note also that at the normal operational stress levels, the microstructural damages are also and indirectly accounted for by the pertinent material parameters. Therefore, one may postulate that at the normal operation where stresses are significant, then the first term (i.e., the strain energy density) in Eq. (14) is dominant and responsible for the damage in the material. On the other hand, as material is subjected to heat in absence of mechanical loading and constraints, the stresses are reduced and approach zero. This would cause W_t to be dominant and responsible for the damage. Previous investigations [19, 20] indicate that this postulation is valid. To obtain W using Eq. (14) then one needs first to compute the stresses and strains as functions of time up to the rupture time. For simple cases this may be achieved analytically and for more complex cases a numerical method such as FEM may be employed. In determining the stress and stain fields as functions of time, the creep constitutive relationships up to the point of rupture including any tertiary region must be used, i.e., the model requires the inclusion of the creep tertiary response in the constitutive equation, which is normally obtained from uniaxial creep tests. If the tertiary creep response from uniaxial creep tests is not available, one can include the effects of the tertiary creep in the constitutive equation by suddenly increasing the creep strains at the uniaxial time-to-rupture (see Section 4 below). These data are part of the essential ingredients of any analysis involving creep deformation and normally obtained from the uniaxial creep tests. If no direct material data are available, published generic data may be utilized, with appropriate sensitivity analyses to cover the uncertainties. Note that in a creep finite element analysis, small time increments within the tertiary region and near the component rupture time are

usually required but almost any finite element program with creep analysis capability that uses an inherent time integration algorithm may be used for this task - see, for example, Zarrabi and Hosseini-Toudeshky [21, 22]. In FEM, however, there will be a time at which a solution might not be converged for even very small time increments indicating the creep failure point of the component has been reached. Therefore, the model proposes that the computed W versus t graph be monitored. Referring to this graph, the proposed model characterises the component failure when $\frac{dW}{dt} \to \infty$ (or $\frac{dt}{dW} \to 0$), see also Section 4.

4. Verification of the proposed model

Brown [23] conducted an elastic-plastic-creep testing on a closed-ended thick cylindrical vessel at 565 ^{o}C and experimentally determined the rupture time of 9000 hours. Also, Brown [24] carried out different tests for welded cylindrical vessels at 565 ^{o}C and experimentally determined the rupture time of 22.039 hours when the tube parent material (PM) was 0.5%Cr-0.5%Mo-0.25%V steel whereas the material of its weld was 2.25%Cr-1%Mo steel. A fine axisymmetric FE mesh was generated to model the creep and damage behavior of the pipe and to obtain the failure life. ANSYS code [25] was used for the finite element analysis with a FORTRAN code developed by the author to link the creep constitutive equations defined by Eqs. (15) and (16) to ANSYS code. The uniaxial creep rupture data [23] was defined by Eq. (17) for the thick tube, as for the welded tube three constitutive equations were implemented [24]. Equation (18) represents the PM, equation (19) represents the HAZ, and equation (20) represents the weld. FE creep damage analyses were performed for the pressurized vessels using the creep constitutive equations of each material which are represented by Eqs. (15) and (16):

$$\dot{\varepsilon}^c = B\sigma^n \quad \text{if} \quad t \le t_r, \tag{15}$$

$$\dot{\varepsilon}^c = mB\sigma^n \quad \text{if} \quad t \ge t_r. \tag{16}$$

Here B was the creep stress coefficient, n was the Norton stress index, t_r as the uniaxial time-to-rupture and the factor $m \ge 5$ was a constant. The values of B and n are listed in Section 4.1 and 4.2 respectively; and they were average values obtained from uniaxial creep data reported graphically by Brown *et al*. [23, 24]. These values when used in Eqs. (15) and (16) with stress in MPa gave creep strain rate in unit of mm/mm/hour. To describe the tertiary creep stage the factor $m = 10$ is included to represent a relative sudden increase in strain rate as the time-to-rupture is approached. It is worth noting that the actual value of m is somewhat arbitrary and the authors assumed that choosing $m = 10$ is sufficient to impose a sudden increase in the creep strain rate when $t \ge t_r$ at a critically loaded point in the material to indicate the tertiary damage.

4.1. Thick Tube. The closed-ended thick cylindrical vessel was subjected to a uniform internal pressure of 106.67 MPa. This experimental load that was used by Brown [23] was employed for finite element analysis (Fig. 3).

The finite element model included the uniform end traction of 35.56 MPa to simulate the end loading due to internal pressure. The vessel had an internal diameter of 20.00 mm and external diameter of 40.00 mm and it was 100 mm long but because of symmetry half of its length was modeled for finite element analysis, see Fig. 3. Five thousand and ten 8-node axisymmetric elements, including 30 elements in the radial (R) direction and 167 elements in the axial (Z) direction were used to generate the mesh as shown in Fig. 3. The vessel was

made of 0.5%Cr-0.5%Mo-0.25%V steel and its uniaxial stress-strain values at the operating temperature of 565 ^{o}C that was used in the FE analysis are presented in Table 3.

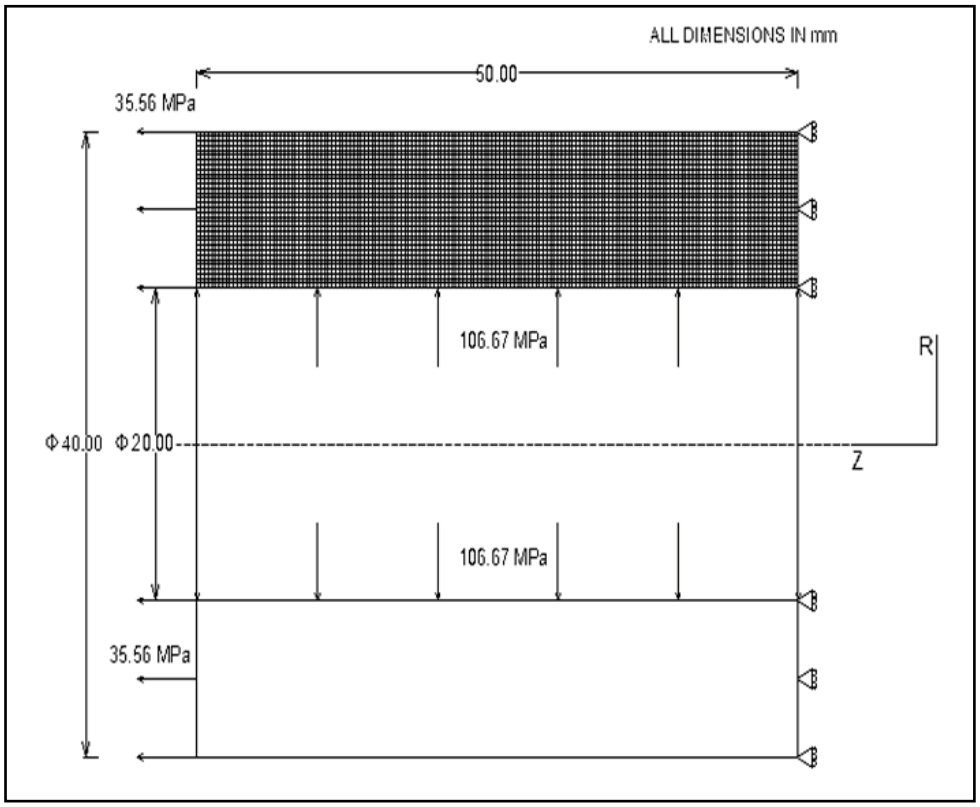

Fig. 3. Dimensions, loading, and finite element model of the vessel.

Table 3. Mechanical tensile properties [16].

At 565 ^{o}C	$E\times10^{6}$, MPa	ν	σ_{y}, MPa	$\varepsilon_{y}\times10^{-4}$	σ_{UTS}, MPa	$\varepsilon_{UTS}\times10^{-2}$
0.5%Cr-0.5%Mo-0.25%V steel	0.1542	0.3	109.5	7.1	143	2.5
2.25%Cr-1%Mo steel	0.1542	0.3	83	5.38	190	2.1

Where $B=107\cdot10^{-30}$ was the creep stress coefficient, $n=11.87$ was the Norton stress index, t_r is the uniaxial time-to-rupture and the factor $m\geq5$ is a constant. The uniaxial rupture data was defined by following equation [23]:

$$\sigma=-48.78751\log_{10}t_r+349.09\,. \tag{17}$$

Figures 4 and 5 show the distributions of the hoop and von Mises equivalent stresses computed using an elastic-creep analysis respectively. For comparison, Figures 6 and 7 show the distributions of the hoop and von Mises equivalent stresses computed using an elastic-plastic-creep analysis respectively. Here, the initial elastic stresses are redistributed by the initial plastic deformation. As a consequence, there is no significant stress redistribution due to the follow-up creep deformation and the variations of stresses with time is minimised. Referring to Figs. 6 - 8, it is apparent that no skeletal stress could accurately be defined for the

elastic-plastic-creep. Figures 6 and 7 show that while hoop stress at the inner surface was lower than the hoop stress at the outer surface, the reverse was true for the von Mises equivalent stress. This was due to high negative compressive (see Fig. 8) radial stress at the inner surface and zero radial stress at the outer surface that would affect the von Mises stress distribution.

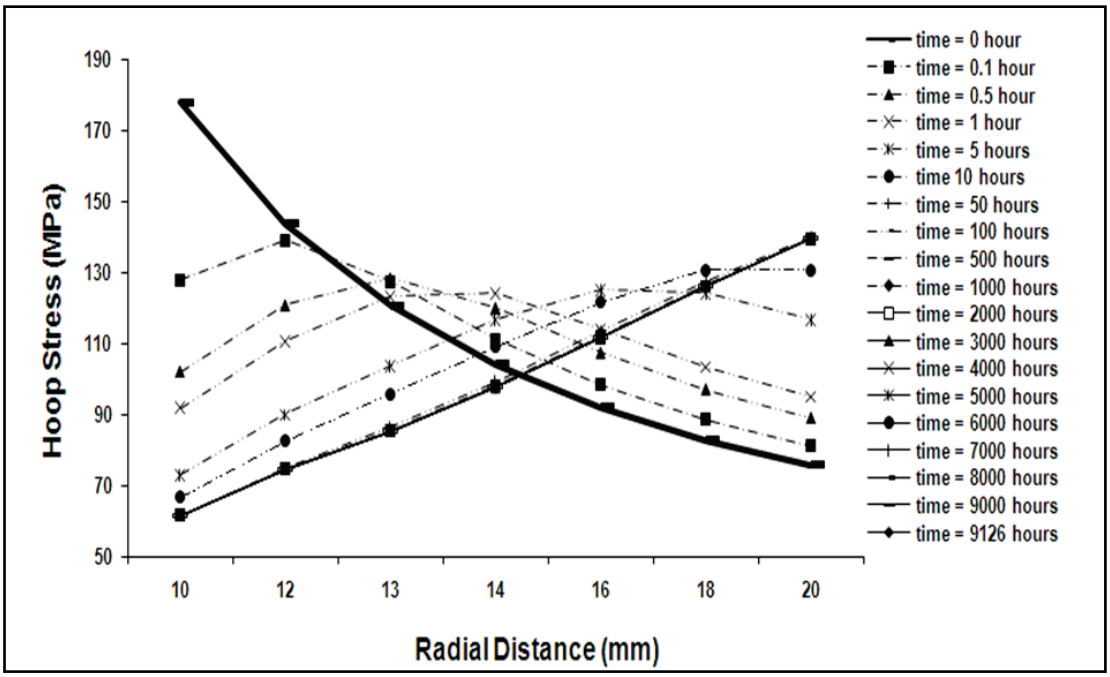

Fig. 4. Hoop stress versus radial distance at various time points computed using an elastic-creep analysis.

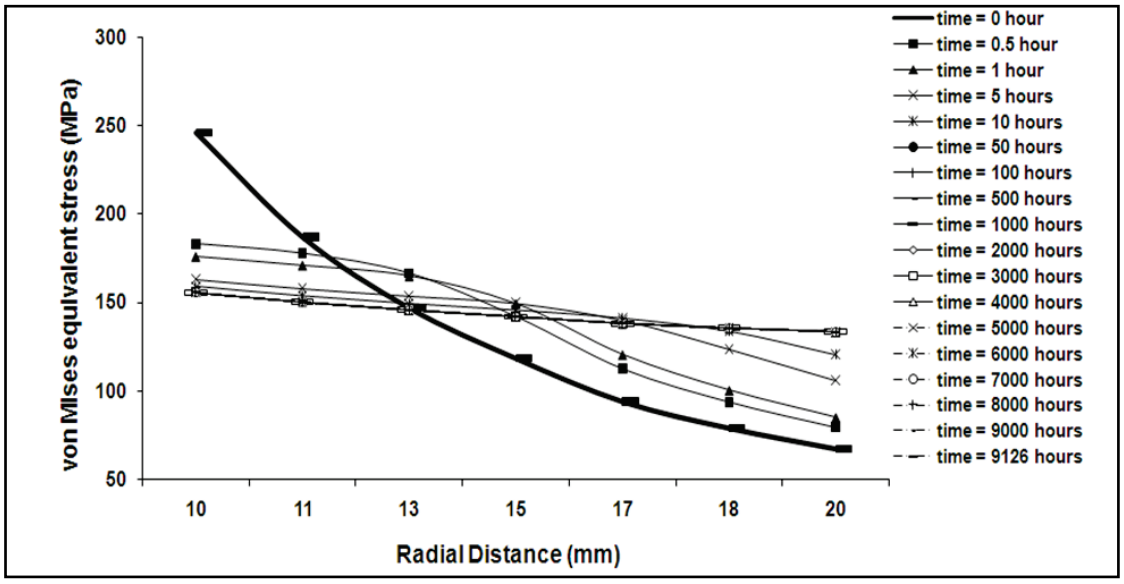

Fig. 5. Von Mises equivalent stress versus radial distance at various time points computed using an elastic-creep analysis.

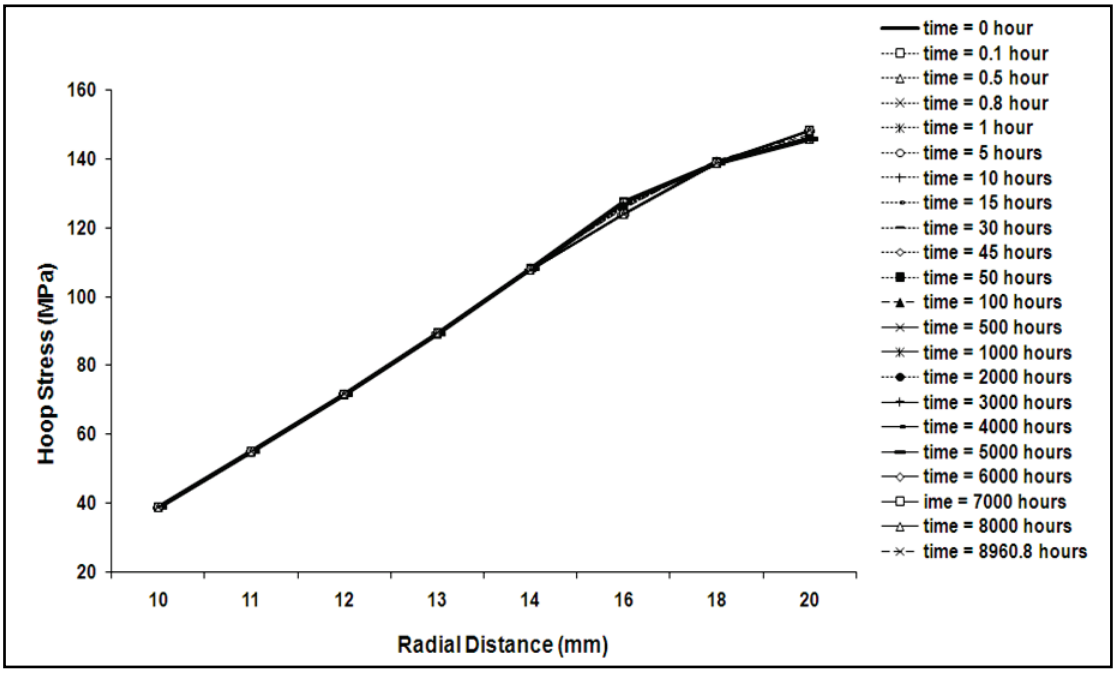

Fig. 6. Hoop stress versus radial distance at various time points computed using an elastic-plastic-creep analysis.

The maximum strain energy density occurred at the inner surface wall of the vessel within element 5678 (see Fig. 9) where the creep damage stain energy density accumulates. The variation of which with time is depicted in Fig. 10. Using the data shown in Fig. 10 and the proposed paradigm, the life of the vessel is predicted as 8961 hours, see also Table 4.

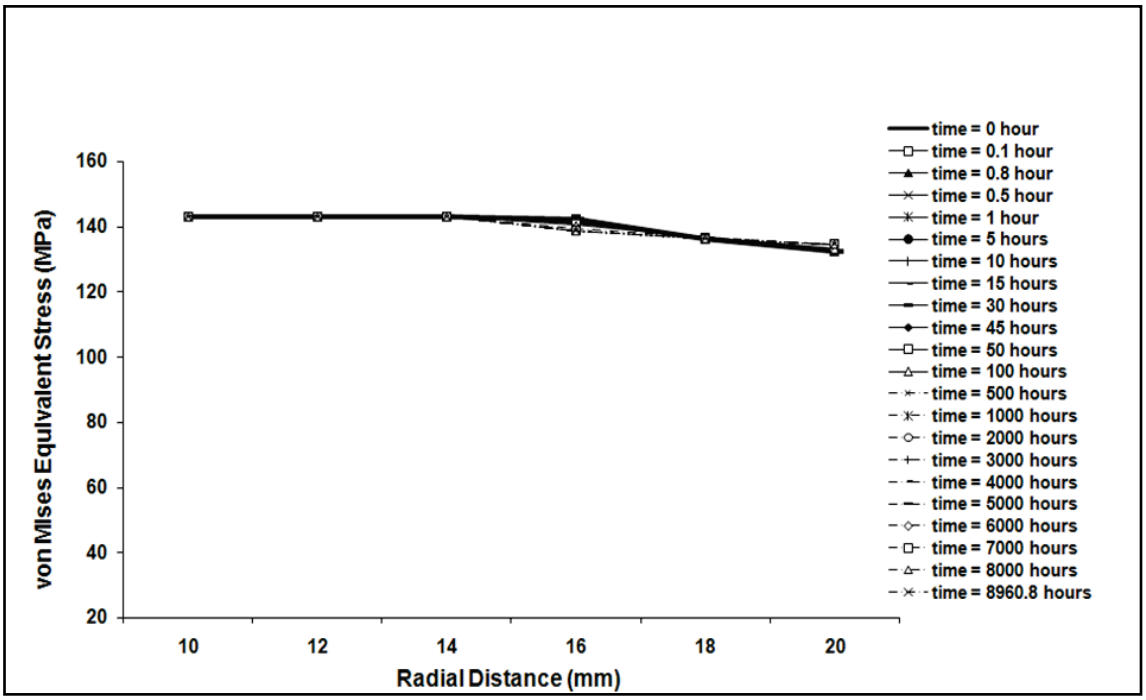

Fig. 7. Von Mises equivalent stress versus radial distance at various time points computed using an elastic-plastic-creep analysis.

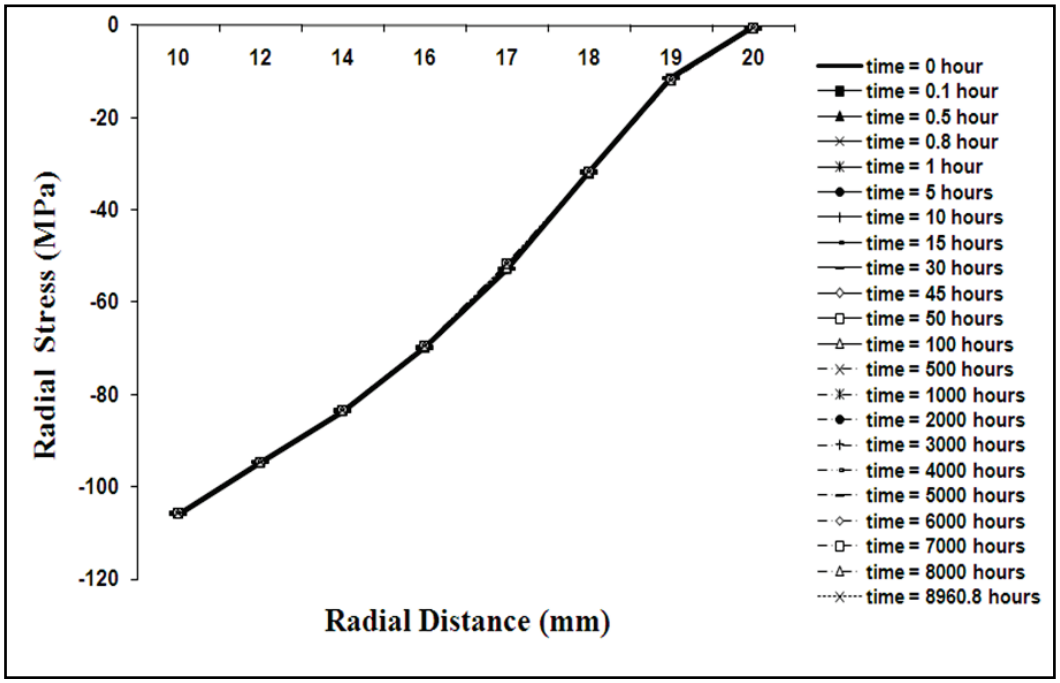

Fig. 8. Radial stress versus radial distance at various time points computed using an elastic-plastic-creep analysis.

Figure 10 shows that the total strain energy density damage implemented by the user-creep code, successfully predicts the same damage evolution with time as the isotropic Norton Creep Law for elastic-creep case within the same element number 5678 (see Fig. 9) in the multiaxial case. Similarly, the user-creep predicted the same total strain energy density for the elastic-plastic-creep case with the same growth damage time as the isotropic Norton Creep damage. These results verify the implementation of the multiaxiality aspect of the implemented user-creep.

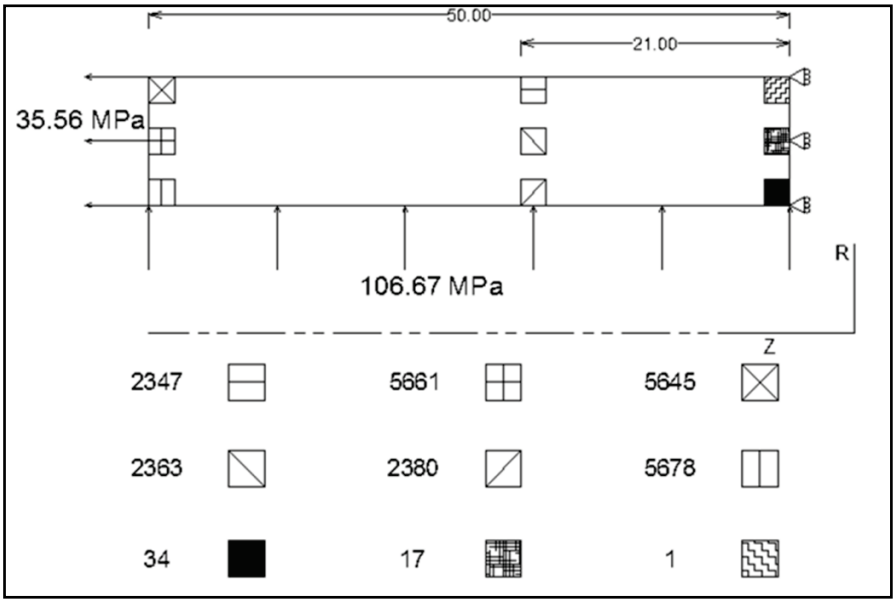

Fig. 9. Configurations of the elements for the thick tube using 8 nodes – axisymmetric element.

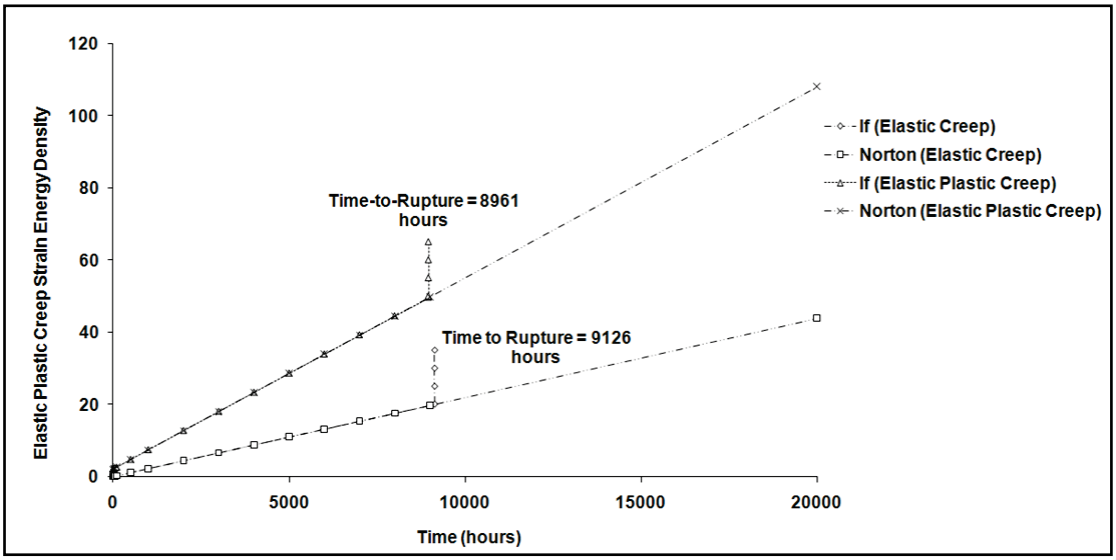

Fig. 10. Total strain energy density versus time at the inner surface of the vessel.

Figure 11 shows the variation of life with Norton creep law index (n). It is obvious that any uncertainties in the pertinent material properties, loading and geometry and dimensions of the component can substantially increase the error in the predicted lives of the components. For example, for the vessel considered in this paper, the variation of $\pm 10\%$ in creep stress index (n) can affect the life of the vessel by a factor of 2, see Fig. 11. Therefore, depending on the uncertainties in the required data for a life prediction, one needs to apply appropriate factor of safety to computed life.

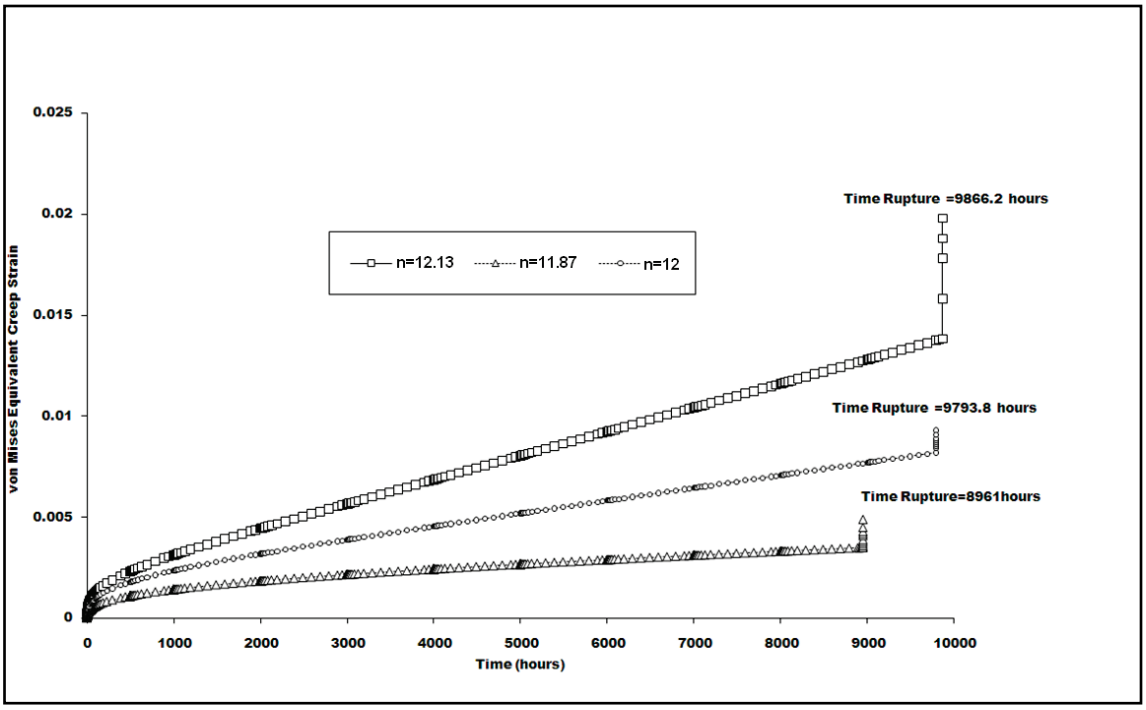

Fig. 11. Variation of life with Norton creep index (n).

Table 4. Lives of vessel predicted using various methods-negative errors indicates a non conservative prediction.

Method		Stress, MPa	Life Predicted, hours	Error,%
Experimental		--	9000	--
Proposed Model (E.P.C.)		--	8961	0.43
Proposed Model (E.C.)		--	9126	-1.4
Reference Stress (Eq.(3))		133	26520	-195
Skeletal Stress (E.P.C.)		σ_{vM} = N/A	--	--
		σ_{hoop} = N/A	--	--
Skeletal Stress (E.C.)		σ_{vM} =150	12044	-34
		σ_{hoop} =110	79550	-784
Robinson Rule (E.P.C.)[26]		σ_{vM}	28661	-30
		σ_{hoop}	32767	-44
Robinson Rule (E.C.)[26]		σ_{vM}	13577	38
		σ_{hoop}	32768	-49
RCC-MR	ECCC	132	9850	-9
	NRIM	132	4837	46
	(Eq.(17))	132	28106	-21
R5		154	9973	-11

4.2. Thick Tube with a central circumferential weld. The closed-ended thick tube with a central circumferential weld (Fig. 12) was made of 0.5%Cr-0.5%Mo-0.25%V steel for PM whereas the material of its weld was 2.25%Cr-1%Mo steel. The mechanical tensile properties of these materials at the test temperature of 565 ^{o}C are shown in Table 3. The finite element model included the uniform end traction of 34.43 MPa to simulate the end loading due to internal pressure. The tube had an internal diameter of 230.00 mm and an external diameter of 350.00 mm and it was 270 mm long but because of symmetry half of its length (360 mm) was modeled for finite element analysis, see (Fig. 12). Three thousand two hundred and eighty six 8-node axisymmetric elements were used to model the tube, with 560 elements in the WM and 185 elements in the HAZ. Elements size in PM varied from 2 mm to 5 mm, and it was 0.75 mm in HAZ and 1 mm in the weld.

Table 5. Uniaxial creep data [24].

Creep Properties	n	B
PM	8.831	$8.1283\cdot10^{-19}$
HAZ	6.267	$1.34896\cdot10^{-14}$
WM	7.514	$1.40929\cdot10^{-15}$

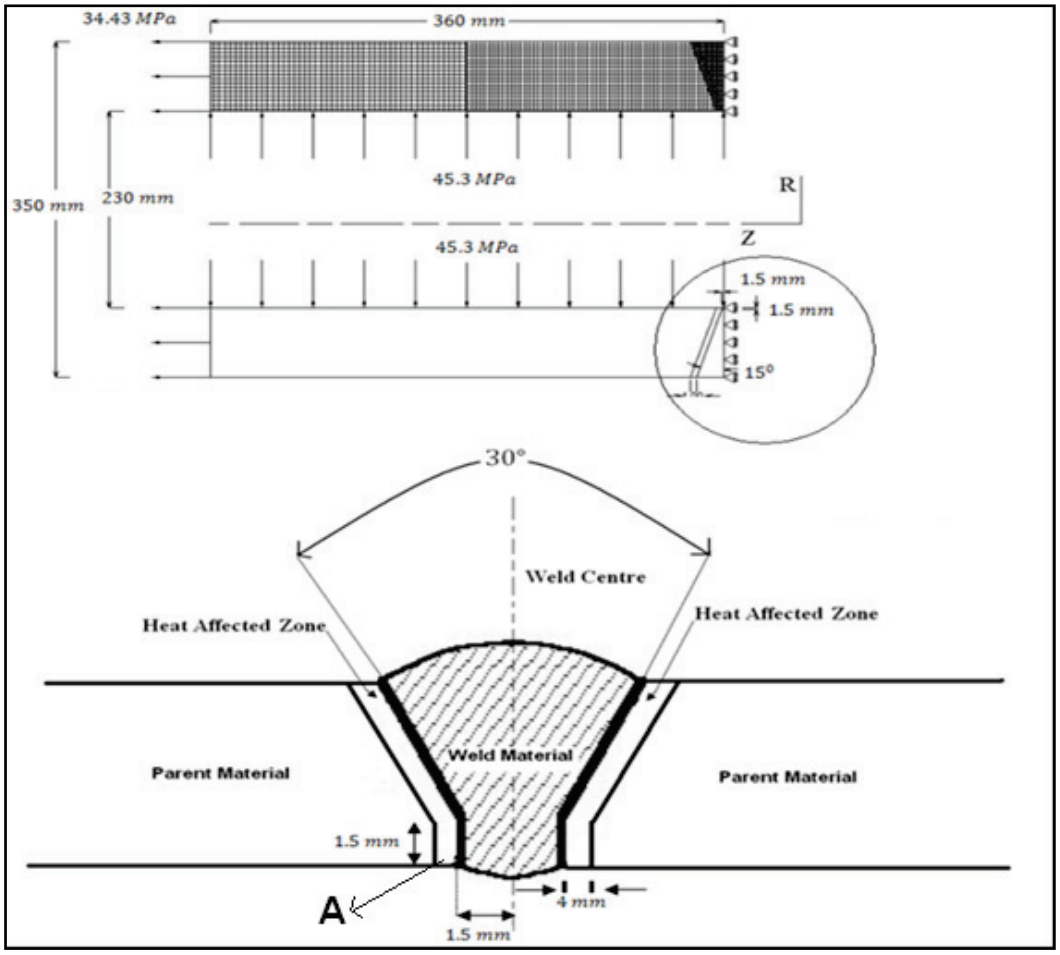

Fig. 12. The geometry and finite element model of the tube.

The values of B and n listed in Table 5 were average values obtained from uniaxial creep data reported graphically by Brown *et al*. [24]. The uniaxial creep rupture data was defined by Eq. (18) for PM, Eq. (19) for HAZ and Eq. (20) for the WM:

$$\sigma_r = -37.66 \log_{10}(t_r) + 299.84, \tag{18}$$

$$\sigma_r = -49.9 \log_{10}(t_r) + 386.94, \tag{19}$$

$$\sigma_r = -38.08 \log_{10}(t_r) + 272.01. \tag{20}$$

The total strain energy density being a measure of plastic-creep damage was highest at the inner surface of the tube, and Figures 13 and 14 show the distributions of the total strain energy densities at the inner surface of the tube at $t = 0$ hour and near the rupture time. Figures 15 to 16 show the distributions of stresses and total von Mises equivalent strains at the inner surface of the tube at $t = 0$ and near the rupture time respectively. Referring to Fig. 13, it is apparent that initially the total strain energy densities were higher in PM and HAZ than those in the weld. Also, at $t = 0$, the equivalent stress in PM and part of HAZ at the inner surface of the tube had just reached yield strength indicating plastic deformation in these regions (Fig. 15). With the passage of time and due to creep and further plastic deformation, the total strain energy density (Fig. 14) were transferred from PM to HAZ causing further

plastic and creep deformation in HAZ. This was also true regarding the total strain energy density that was a measure of damage in the material (see Figs. 13, 14). This resulted in the highest total strain energy density (damage) accumulating at the inner surface and in HAZ causing eventual failure of the tube at point A, (see Figs. 12, 14 for location of point A). The predicted failure location marked by point A correlated well with the HAZ cracking experimentally observed by Brown *et al*. [24]. It is worth noting that stresses followed the same pattern as the total strain energy densities (Fig. 16). However, the strains were accumulating at higher rate in PM away from the welded joint presumably due to less constraint in this region of the tube (Fig. 18). The variation of the maximum total strain energy density (that occurred at point A) with time is depicted in Fig. 23. Using the data shown in Fig. 23 and the proposed model the life of the tube is predicted as 18527 hours (see Tables 6, 7, and 8). Tables 8 and 9 also include the life of the tube estimated according to R5, Robinson time fraction rule [26], reference stress and the RCC-MR life assessment creep design code for comparison. Figures 19 and 20 show the redistribution of the hoop stress and the von Mises equivalent stress in HAZ for various creep times along the wall thickness of the tube using an elastic-creep analysis. It is clear that the stresses at a particular point within the pipe wall are constant with time as would be expected from the skeletal point concept discussed by Marriott *et al.* [8]. Comparing Figs. 18 and 19, it can be seen, that the stress increase with time at the inner surface of the heat-affected-zone (HAZ) while it decrease at the outside surface for the von Mises equivalent stress (see Fig. 19), however, the hoop stress field appears to be more strongly dependent on the creep stress exponent "n" where the stress increases with the increase of radius and remains approximately constant from elastic to steady state creep conditions. In all cases, the rupture stress position was near the inner surface of tube where the damage calculation results have been performed to predict the time-to-rupture (refer to Tables 8, 9, and 10). For comparisons, Figures 21 and 22 show the stress redistribution of the hoop and von Mises equivalent stress across the tube radius for an elastic-plastic-creep analysis. It is clear that the skeletal point concept is not applicable. This is due to the stresses redistribution by the initial plastic deformation. As a consequence, there is no significant stress redistribution due to the follow-up creep deformation and the variations of stresses with time is minimised.

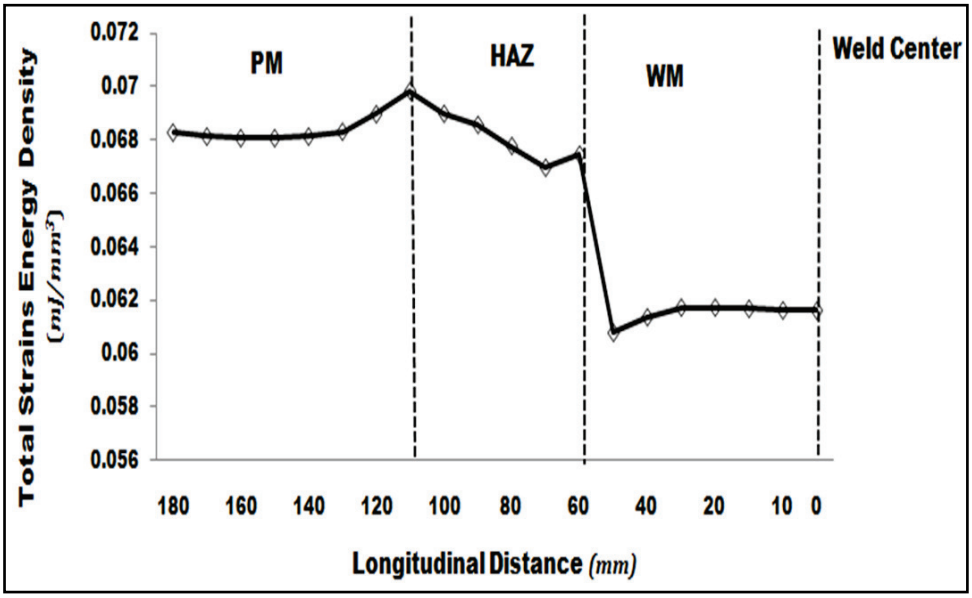

Fig. 13. Total strain energy density distributions at the inner surface of the tube at $t = 0$ hours.

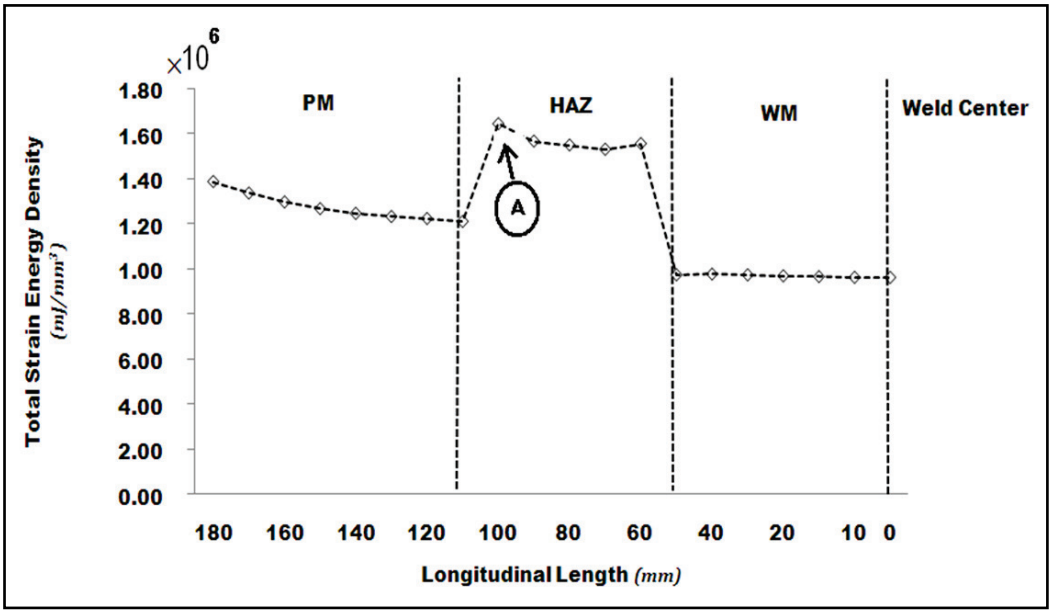

Fig. 14. Total strain energy density distributions at the inner surface of the tube at $t_r = 18527$ hours.

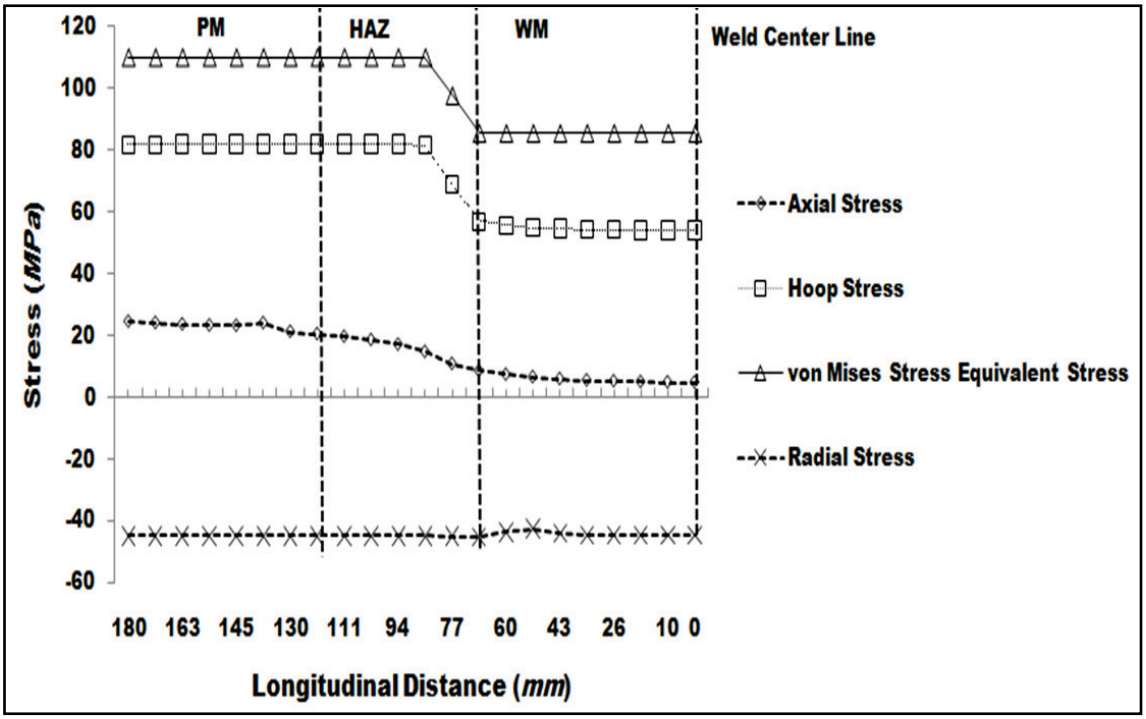

Fig. 15. Stress distributions at the inner surface of the tube at $t = 0$ hours.

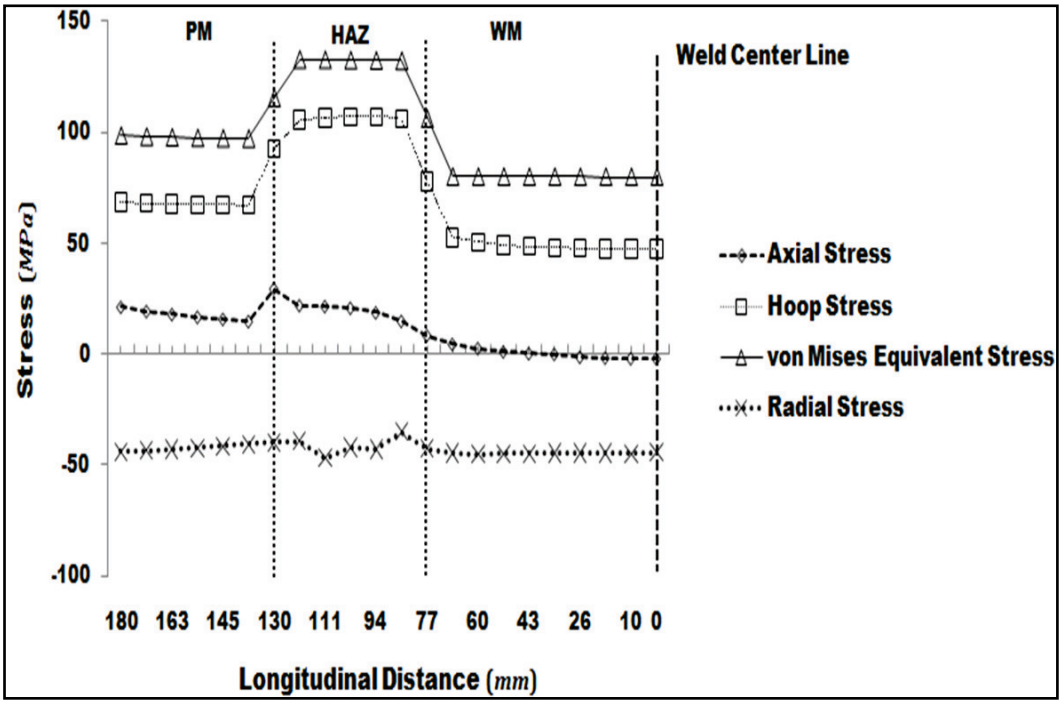

Fig. 16. Stress distributions at the inner surface of the tube at $t_r = 18527$ hours.

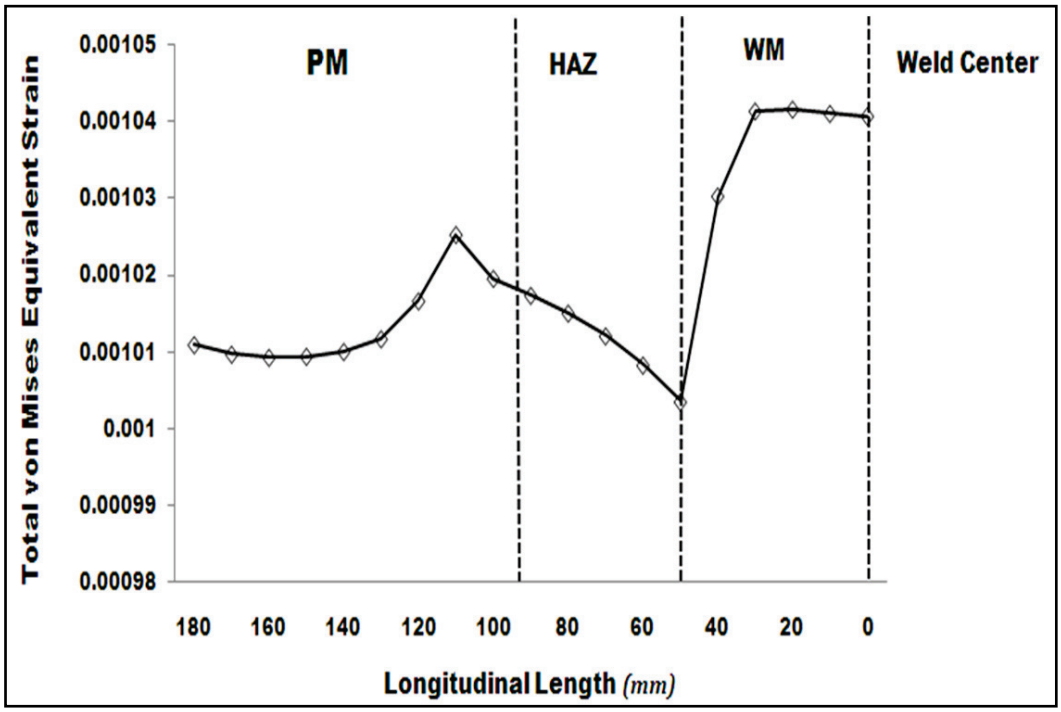

Fig. 17. Total von Mises equivalent strain distributions at the inner surface of the tube at $t = 0$ hours.

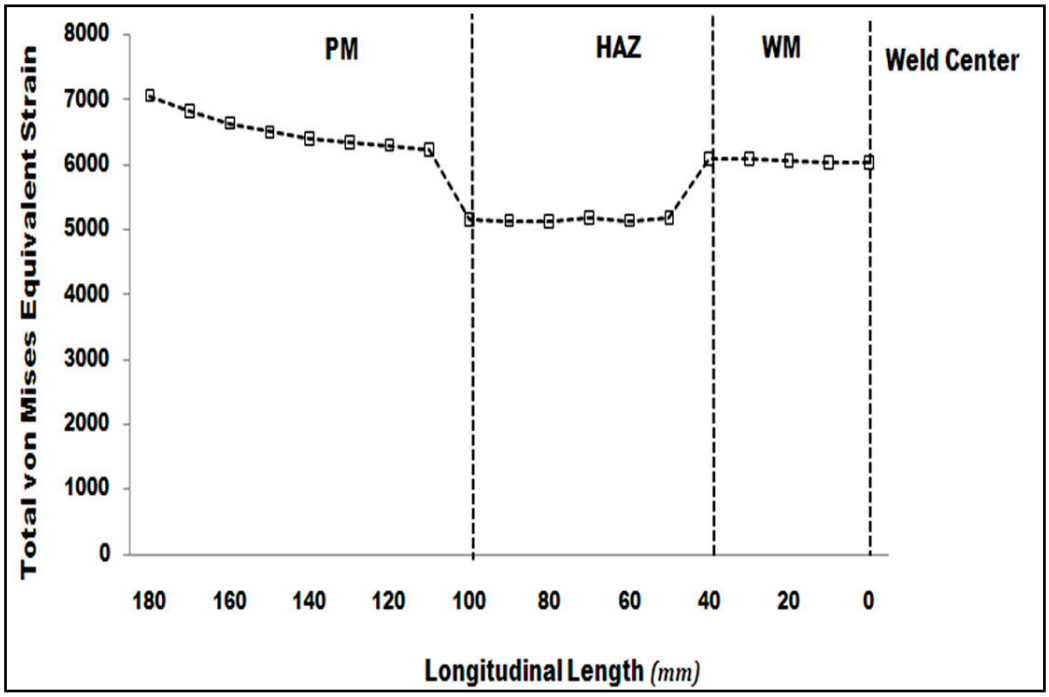

Fig. 18. Total von Mises equivalent strain distributions at the inner surface of the tube at $t_r = 18527$ hours.

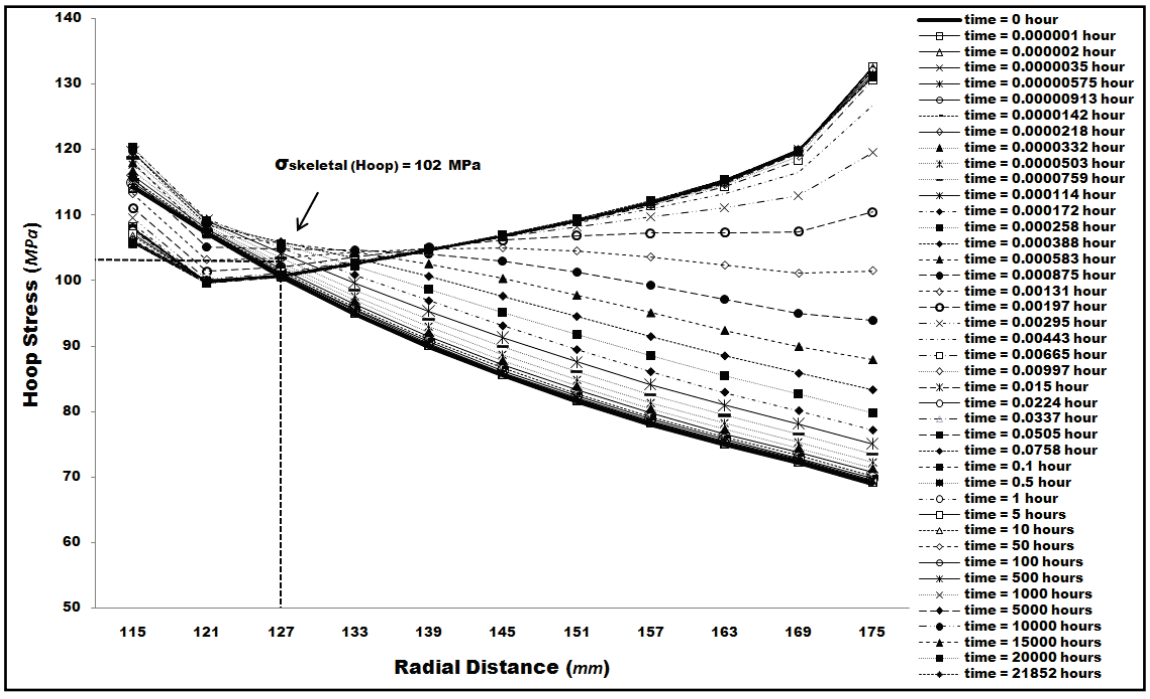

Fig. 19. Hoop stress versus radial distance at various time points computed using an elastic-creep analysis (HAZ).

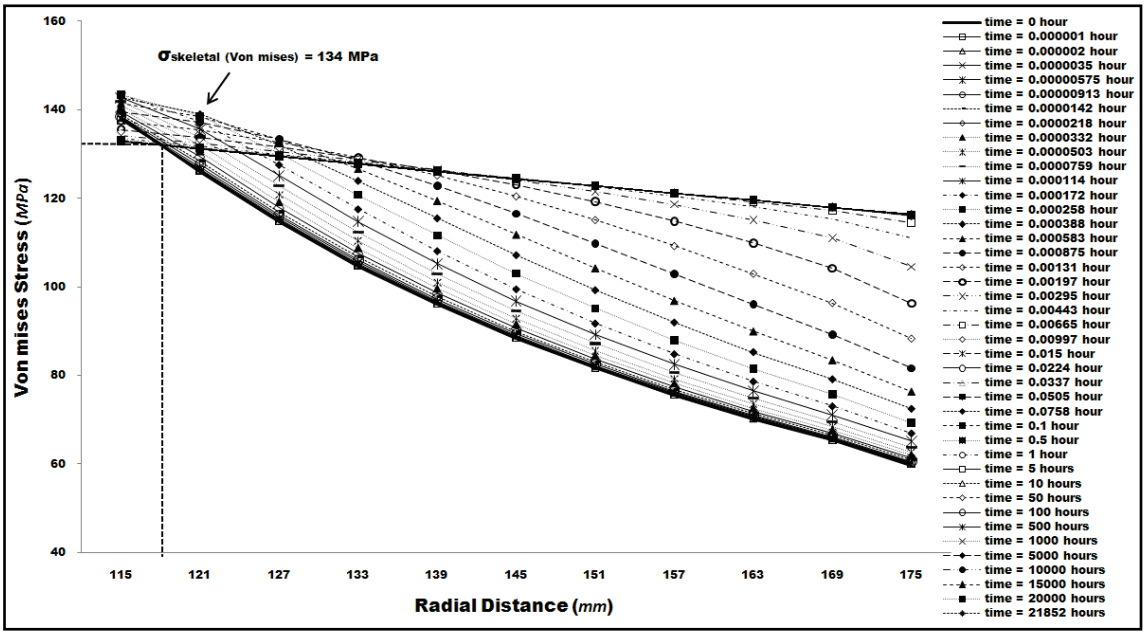

Fig. 20. Von Mises equivalent stress versus radial distance at various time points computed using an elastic-creep analysis (HAZ).

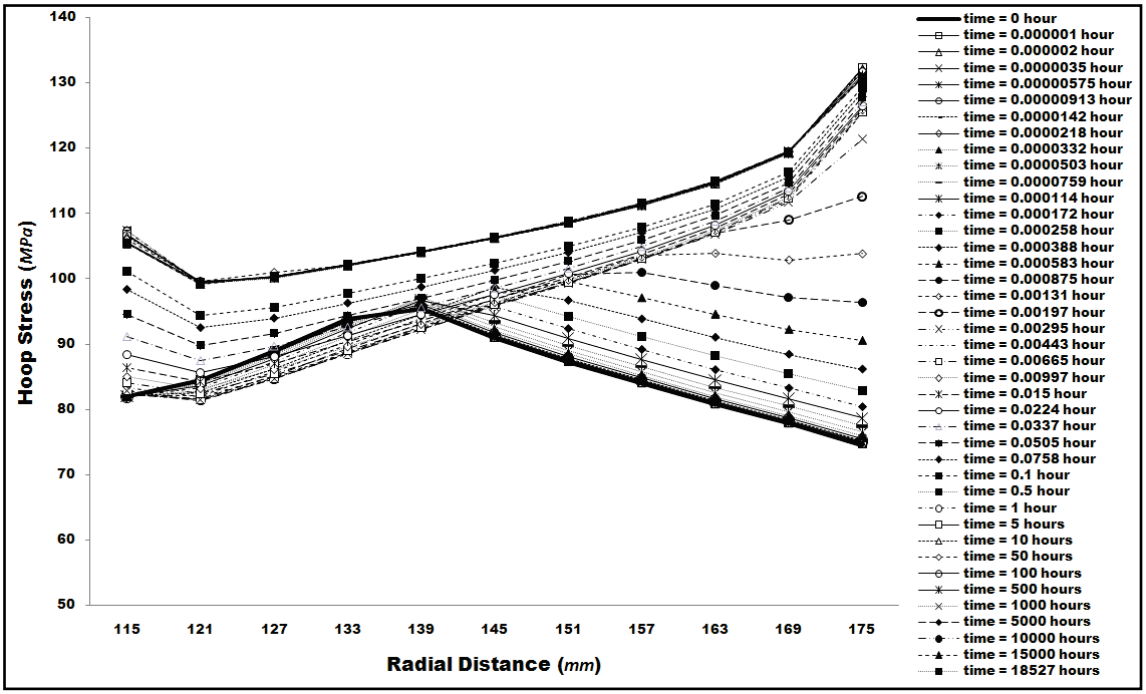

Fig. 21. Hoop stress versus radial distance at various time points computed using an elastic-plastic-creep analysis (HAZ).

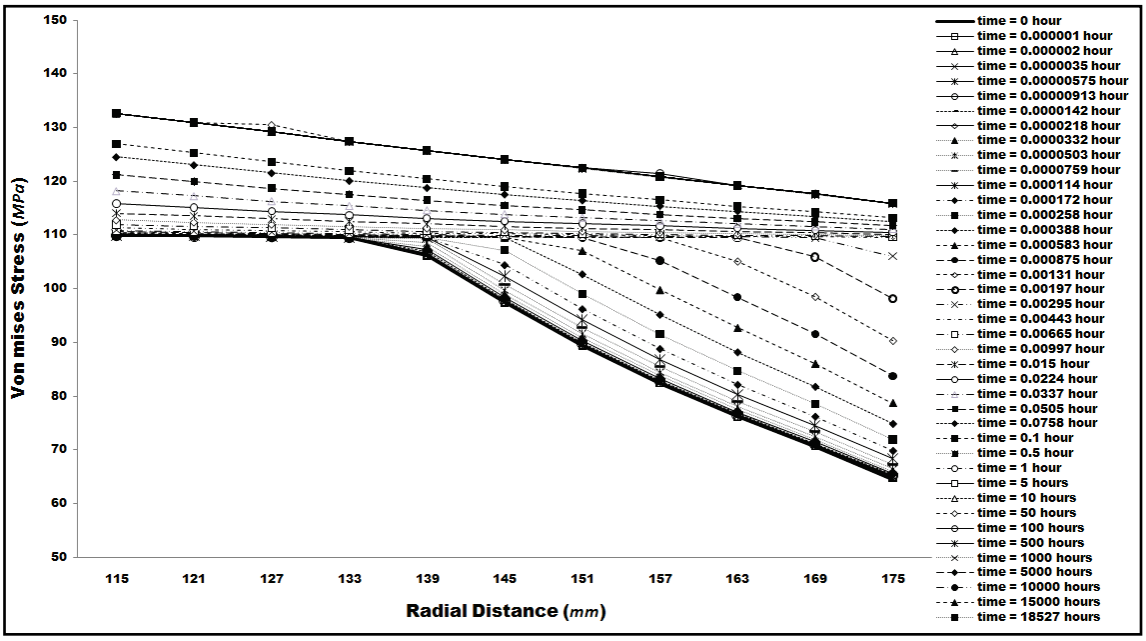

Fig. 22. Von Mises equivalent stress versus radial distance at various time points computed using an elastic-plastic-creep analysis (HAZ).

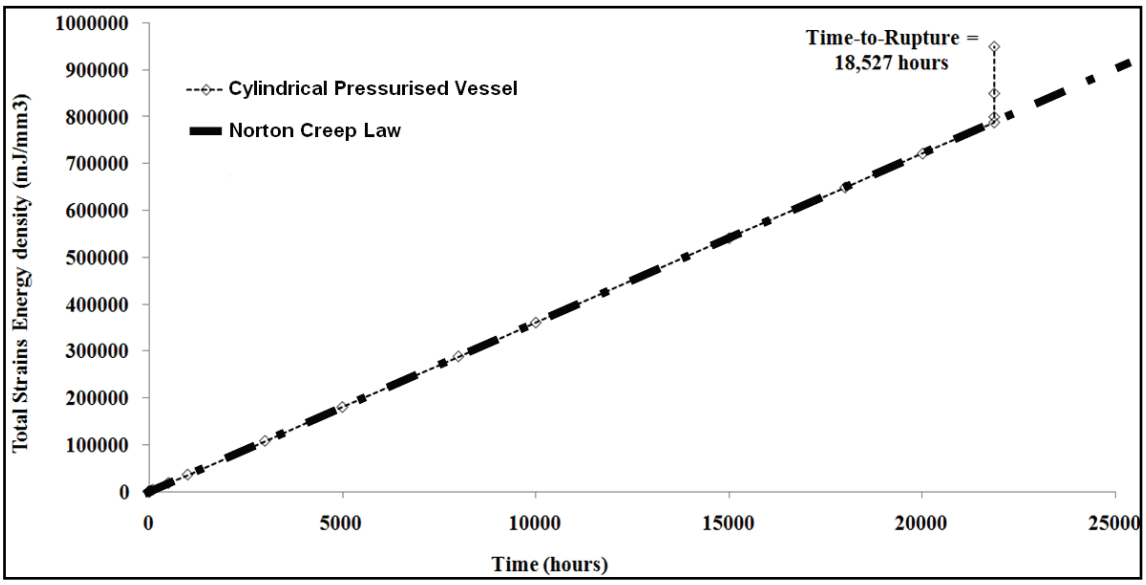

Fig. 23. Variation of the maximum strain energy density occurred at point A with time for an elastic-plastic-creep case.

Table 6. Life of the PM predicted by various models.

Method		Stress, MPa	Predicted Life, hours	Error, %
Experimental		--	22039	--
Proposed Model (E.P.C.)		--	18527	16
Proposed Model (E.C.)		--	21862	0.8
Reference Stress (Eq. (3))		93.43	302609	-1273
Skeletal Stress (E.P.C.)		σ_{vM} =100	202500	-819
		σ_{hoop} =90	373215	-1593
Skeletal Stress (E.C.)		σ_{vM} =100	202500	-819
		σ_{hoop} =90	373215	-1593
Robinson Rule (E.P.C.) [26]		σ_{vM}	36466	-65
		σ_{hoop}	22517	-2
Robinson Rule (E.C.) [26]		σ_{vM}	26600	-21
		σ_{hoop}	13483	39
RCC-MR	ECCC	120	9475	57
	NRIM	120	7943	64
	Eq. (18)	120	63096	-186
R5		133.24	26517	-20

(Note: Negative errors indicate non-conservative life prediction)

Table 7. Life of the HAZ predicted by various models.

Method	Stress, MPa		Predicted Life, hours	Error, %
Experimental	--		22039	--
Proposed Model (E.P.C.)	--		18527	16
Proposed Model (E.C.)	--		21862	0.8
Reference Stress (Eq. (3))	93.43		762016	-3358
Skeletal Stress (E.P.C.)	$\sigma_{V.M}$ = N/A		--	--
	σ_{hoop} = N/A		--	--
Skeletal Stress (E.C.)	$\sigma_{V.M}$ =134		117203	-432
	σ_{hoop} =102		513122	-2228
Robinson Rule (E.P.C.) [26]	$\sigma_{V.M}$		43186	-100
	σ_{hoop}		33997	-54
Robinson Rule (E.C.) [26]	$\sigma_{V.M}$		40731	-85
	σ_{hoop}		33308	-51
RCC-MR	ECCC	120	9475	57
	NRIM	120	7943	64
	Eq. (19)	120	199526	-805
R5	133.24	121.386	-451	

(Note: Negative errors indicate non-conservative life prediction.)

Table 8. Life of the WM predicted by various models.

Method	Stress, MPa		Predicted Life, hours	Error, %
Experimental	--		22039	--
Proposed Model (E.P.C.)	--		18527	16
Proposed Model (E.C.)	--		21862	0.8
Reference Stress (Eq. (3))	93.43		48933	-122
Skeletal Stress (E.P.C.)	σ_{vM} =74		158432	-620
	σ_{hoop} = 81		103757	-371
Skeletal Stress (E.C.)	σ_{vM} =77		132148	-500
	σ_{hoop} =37		1484161	--
Robinson Rule (E.P.C.) [26]	σ_{vM}		24103	-9.3
	σ_{hoop}		8391	62
Robinson Rule (E.C.) [26]	σ_{vM}		15514	30
	σ_{hoop}		5941	73
RCC-MR	ECCC	133	4536	79
	NRIM	133	6457	71
	Eq. (20)	133	20276	8
R5	133.24		4407	80

(Note: Negative errors indicate non-conservative life prediction)

5. Conclusions

This paper proposed an accurate and pragmatic paradigm for predicting lives of components subjected to elastic-plastic-creep deformation. The model is based on multiaxial stress and strain fields and as such takes into accounts the internal forces and deformation in the material. The proposed model does not require material parameters (e.g., α) whose evaluation is awkward and/or uneconomic. It was shown that the model predicts the life with good accuracy, i.e., less than 5% for the elastic-creep case for the welded tube and less than 20% for the elastic-plastic-creep case. It is obvious that any uncertainties in the pertinent material properties, loading and geometry and dimensions of the component can substantially increase the error in the predicted lives of the components. There are several uncertainties in design of high temperature components including load uncertainty, material property uncertainty and analysis approximations. Note also that the applicable material data for creep analysis are usually obtained from complex high-temperature testing. As a result, the pertinent material data and experimentally determined lives may be contaminated with scatter. The present study is concerned with the effect of material data on creep damage models. Normally these models contain parameters whose values have a certain level of uncertainty. In order to ease this problem, appropriate sensitivity analysis can be conducted to cover all these uncertainties (see Tables 9 - 11). For example, for the welded cylindrical vessel considered in this paper, the variation of $\pm$5% in creep stress index (n) can affect the life of the vessel. Therefore, depending on the uncertainties in the required data for a life prediction, one needs to apply appropriate factor of safety to the computed life. Table 9 summarized the values for the PM when the stress exponent varied from 8.2289 to 9.0951 ($\pm$5%), based on the creep

material data. This results in a variation of 100000 to 6517 hours (or -353.74% to 70.43%). Table 10 varied from 5.72945 to 6.33255 (± 5%) based on the creep material data for HAZ. This results in a variation of 48373 to 49597 hours (or -119.49% to -125.04%). Table 11, the stress exponent "n" is varied from 7.4765 to 8.2635 (± 5%) based on the creep material data of WM. This results in a variation of 47510 to 50096 hours (or -115.574% to -127.31%).

Table 9. Variation of "n" for PM for an elastic-plastic-creep case.

0.5%Cr-0.5%Mo-0.25%V PM	Experimental Life, hours	Predicted Life (hours)	% Δ_{Life}	n_p	n_o	% Δ_n	B_0, $\frac{1}{hour}/MPa^n$
	22039	48638	-120.69		8.662		$8.13\cdot10^{-19}$
5%MIN of "n"	22039	100000	-353.74	8.2289	8.662	-5.00	$8.13\cdot10^{-19}$
5%MAX of "n"	22039	6517	70.43	9.0951	8.662	5.00	$8.13\cdot10^{-19}$
SENSITIVITY ANALYSIS	22039	18.527	16	8.831	8.662	1.95	$8.13\cdot10^{-19}$

Table 10. Variation of "n" for HAZ for an elastic-plastic-creep case.

0.5%Cr-0.5%Mo-0.25%V HAZ	Experi-mental Life, hours	Predicted Life, hours	% Δ_{Life}	n_p	n_o	% Δ_n	B_0, $\frac{1}{hour}/MPa^n$
	22.039	48.638	-120.69		6.031		$1.35\cdot10^{-14}$
5%MIN of "n"	22.039	48.373	-119.49	5.72945	6.031	-5.00	$1.35\cdot10^{-14}$
5%MAX of "n"	22.039	49.597	-125.04	6.33255	6.031	5.00	$1.35\cdot10^{-14}$
SENSITIVITY ANALYSIS	22.039	18.527	16	6.267	6.031	3.91	$1.35\cdot10^{-14}$

It is obvious from Tables 9-11 that the effect of the creep material properties, within the PM, HAZ and WM, affect the life of the tube where high stresses and damage accumulation can be observed in the heat-affected-zone (HAZ). This is due to the mismatch of the stress exponent *"n"*and the stress coefficient obtained from the scattered which leads to a difficulty to predict the stress concentration and to establish the accurate life of the pressurised vessel which is influenced by the multi-axiality stress/strain.

Table 11. Variation of "n" for 2.25Cr-1Mo (WM) for an elastic-plastic-creep case.

2.25Cr-1Mo WM	Experimental Life, hours	Predicted Life, hours	% Δ_{Life}	n_p	n_o	% Δ_n	B_0, $\frac{1}{hour/MPa^n}$
	22039	48638	-120.69		7.87		$1.41 \cdot 10^{-15}$
5% MIN of "n"	22039	47510	-115.57	7.4765	7.87	-5.00	$1.41 \cdot 10^{-15}$
5% MAX of "n"	22039	50096	-127.31	8.2635	7.87	5.00	$1.41 \cdot 10^{-15}$
SENSITIVITY ANALYSIS	22039	18527	16	7.514	7.87	-4.52	$1.41 \cdot 10^{-15}$

Although the weld was manufactured using a specialized welding procedure [24, 27] to ensure robust weld metal and to obtain the rupture location in the HAZ which is consider it to be the weakest zone within the vessel, where the damage will be accumulated within this critical zone, the plastic deformation still play a significant role through the thickness wall of the vessels where the damage variation could be measured by the plastic strain energy density. Also, as Hyde and Sun pointed in [28], the objective of assessing the pressurized vessels subjected to a creep deformation is to predict a perfect match between the creep properties in each of the PM, HAZ and WM. However, such issue would be unfeasible to achieve. Also, ductility is very important for the analysis of an internally pressurized welded pipe, as there will be constraint applied to the weld. This result leads to an advantage in using weld metals that are slightly weaker than the PM [28].

Acknowledgement

The Authors would like to thank Associate Professor Zarrabi for his helpful discussions, information and expert advice given in the area of creep analysis, as well as allowing us to conduct the analysis by using his pragmatic model in order to obtain certain insights into the life assessment prediction for pressure vessels subjected to elastic-plastic-creep deformations.

References

[1] J. Schweiker, O. Sidebottom // *Experimental Mechanics* **5** (1965) 186.
[2] B. Wilshire, P. J. Scharning // *Int. J. Pressure Vessels and Piping* **85** (2008) 739.
[3] S.-T. Tu, R. Wu, R. Sandström // *Int. J. Pressure Vessels and Piping* **58** (1994) 345.
[4] K. Zarrabi, J. Jelwan // *Int. J. Materials Engineering and Technology* **3** (2010) 173.
[5] R. K. Penny, D. L. Marriot, *Design for creep* (Chapman & Hall, London, UK, 1995).
[6] H. F. Chen, Z. Z. Cen, B. Y. Xu, S. G. Zhan. // *Int. J. Pressure Vessels and Piping* **71** (1997) 47.
[7] R. G. Sim // *Int. J. Mech. Sci.* **12** (1970) 561.
[8] D.L. Marriott, F. A. Leckie // *Proc. Inst. Mech. Eng.* **178** (1963-1964) 115.
[9] K. Zarrabi // *Int. J. Pressure Vessels and Piping* **53** (1993) 351.
[10] F. Šiška, J. Aktaa // *Fusion Engineering and Design* **85** (2010) 215.
[11] *R5* (July 1995, Issue 2), Assessment procedure for the High Temperature Response of Structures (Berkeley Technology Center, Nuclear Electric plc., 1995).
[12] J. Shi // *ASME Conference Proceedings* **3** (2009) 953.
[13] Bernard Riou, Morello Sperandio, Claude Escaravage, Bernard Drubay, Marie-Thérèse Cabrillat, Yves Mézière, Bernard Salles, In: *Transactions of the 17th International*

Conference on Structural Mechanics in Reactor Technology (SMiRT 17) (Prague, Czech Republic, 2003) paper # F01-1.
[14] P. Chellapandi, R. Srinivasan, S.C. Chetal, Baldev Raj // *Int. J. Pressure Vessels and Piping* **83** (2006) 556.
[15] F. Abe, W. B., H. Doi, J. Hald, S.R. Holdsworth, M. Igarashi, T.-U. Kern, S. Kihara, K. Kimura, T. Kremser, A. Lizundia, K. Maile, F. Masuyama, G. Merckling, Y. Minami, P.F. Morris, J. O. T. Muraki, R. Sandstrom, J. Schubert, G. Schwass, M. Spindler, M. Tabuchi, K. Yagi, M. Yamada, In: *Creep Properties of Heat Resistant Steels and Superalloys. Numerical Data and Functional Relationships in Science and Technology, Group VIII: Advanced Materials and Technologies,* ed. by K. Yagi, G. Merckling, T.U. Kern, H. Irie, H. Warlimont (Springer-Verlag, Berlin, Heidelberg, New York, 2004) Subvolume B 2.
[16] http://www.nims.go.jp/eng/
[17] T. Mamood, J. Jelwan, K. Zarrabi // *Int. J. Advances in Engineering and lnterdisciplinary Scienlific Research (AES)* (2010) in print.
[18] K. Zarrabi, J. Jelwan, T. Mamood, In: *Proceedings of ASME IMECE, International Mechanical Engineering Congress & Exposition* (Vancouver, British Columbia, Canada, 2010) IMECE2010-37042.
[19] K. Zarrabi, L. Ng // *The International Journal of Science and Technology - Scientia Iranica-Transactionson: Mechanical and Civil Engineering* **14** (2007) 450.
[20] K. Zarrabi, L. Ng // *J. Pressure Vessel Technology* **130** (2008) 041201.
[21] K. Zarrabi, H. Hosseini-Toudeshky // *Int. J. Pressure Vessels and Piping* **62** (1995) 195.
[22] K. Zarrabi, H. Hosseini-Toudeshky, In: *Proceedings of the International Joint Power Generation Conference and Exposition*, ed. by A. Sanyal, A. Gupta and J. Veilleuxn (ASME, New York, Denver, USA, 1997) EC-Vol. 5.
[23] R.J. Browne, In: *Techniques for multiaxial creep testing*, ed. by D.J. Gooch and I.M. How (Elsevier Applied Science, London, New York, 1986).
[24] R.J. Browne, B.J. Cane, J.D. Parker, D.J. Walters, In: *Creep and fracture engineering materials and structures. Proc. of the International Conference held at University College, Swansea, 24th–27th March, 1981*, ed. by B. Wilshire, D.R.J. Owen (Pineridge Press, Swansea, U.K., 1981) p. 645.
[25] *ANSYS* (May 2008), ANSYS Release 12.0 (ANSYS Inc., USA).
[26] E.L. Robinson // *Trans. ASME* **74** (1952) 777.
[27] M.C. Coleman, J.D. Parker, D.J. Walters *// Int. J. Pressure Vessels and Piping* **18** (1985) 277.
[28] T. Hyde, J. Williams, W. Sun // *OMMI: Operation Maintenance and Materials Issues* **1** (3) (2002).